

Received December 24, 2020, accepted December 30, 2020, date of publication January 6, 2021, date of current version January 20, 2021.

Digital Object Identifier 10.1109/ACCESS.2021.3049528

# Dynamic Semiempirical PEMFC Model for Prognostics and Fault Diagnosis

SAAD SALEEM KHAN<sup>1</sup>, HUSSAIN SHAREEF<sup>1</sup>, (Member, IEEE), MOHSEN KANDIDAYENI<sup>2</sup>, (Member, IEEE), LOÏC BOULON<sup>2</sup>, (Senior Member, IEEE), ABBOU AMINE<sup>3</sup>, AND EL HASNAOUI ABDENNEBI<sup>4</sup>

<sup>1</sup>Department of Electrical Engineering, United Arab Emirates University, Al Ain 15551, UAE

<sup>2</sup>Hydrogen Research Institute, Department of Electrical Engineering and Computer Science, Université du Québec à Trois-Rivières, Trois-Rivières, QC G9A 5H7, Canada

<sup>3</sup>Engineering for Smart & Sustainable Systems Research Centre, Mohammadia School of Engineers, Agdal Rabat 10090, Morocco

<sup>4</sup>Electro Mechanics Department, Superior School of Mines, Agdal Rabat 10000, Morocco

Corresponding author: Hussain Shareef (shareef@uaeu.ac.ae)

This work was supported in part by the United Arab Emirates University under Grant 31R067 and in part by the Natural Sciences and Engineering Research Council of Canada (NSERC) under Grant 2018-06527.

**ABSTRACT** This article introduces a dynamic semiempirical model that predicts the degradation of a proton exchange membrane fuel cell (PEMFC) by introducing time-based terms in the model. The concentration voltage drop is calculated using a new statistical equation based on the load current and working time, whereas the ohmic and activation voltage drops are updated using time-based equations borrowed from the existing literature. Furthermore, the developed model calculates the membrane water content in the PEMFC, which indicates the membrane hydration state and indirectly diagnoses the flooding and drying faults. Moreover, the model parameters are optimized using a recently developed butterfly optimization algorithm. The model is simple and has a short runtime; therefore, it is suitable for monitoring. Voltage degradation under various loading currents was observed for long working hours. The obtained results indicate a significant degradation in PEMFC performance. Therefore, the proposed model is also useful for prognostics and fault diagnosis.

**INDEX TERMS** Fault diagnostics, optimization, PEMFC, prognostics, statistical analysis.

## I. INTRODUCTION

Proton exchange membrane fuel cells (PEMFCs) are a promising clean energy source with high energy density and environmental nontoxicity [1]–[3]. The implementation of PEMFCs is primarily limited by their low durability. Generally, PEMFCs have a short-life span, ranging from three years for stationary applications to 3000 h for transportation applications [4], [5]. The causes of PEMFC degradation are listed below.

- (i) Membrane degradation is the outcome of chemical degradation, which leads to the thinning of the membrane and unwanted gas crossover. Membranes are also degraded by mechanical stress, which can lead to cracking and the formation of pinholes. Thermal stress is induced by the high temperatures produced in the PEMFC (above 200 °C).

The associate editor coordinating the review of this manuscript and approving it for publication was Pengcheng Liu<sup>1</sup>.

- (ii) The ionomer in the catalyst layer undergoes degradation during long-term operations, which eventually affects the ionic conductivity of the PEMFC.
- (iii) The gas diffusion layers become degraded by many factors, most importantly owing to the water management in the PEMFC system.
- (iv) Even when the bipolar plates comprise stainless steel, they can become corroded, with consequent degradation of the PEMFC. Carbon corrosion is caused by the presence of water, which produces carbon surface oxides.
- (v) Platinum catalyst degradation occurs during voltage cycling. A steady-state voltage of the PEMFC can slow this process; however, voltage variations are unavoidable in real-time applications. PEMFCs used with super-capacitors or batteries can mitigate this problem to some extent [4], [6]–[12].

To improve the life expectancy of PEMFCs, many studies have adopted improved materials and various monitoring and control systems for PEMFCs. PEMFC health is managed by

performance monitoring of the system, timely diagnosis of faults, degradation assessments, estimation of the remaining useful life, and control of the factors affecting the health of the PEMFC system [13].

Recently, Elodie *et al.* [14] and Lechartier *et al.* [15] reported an aging model for prognostics. They described state-space equations for a dynamic electrical equivalent PEMFC model that calculates the time-dependent voltage. The model was validated in long duration tests of a PEMFC system. Another study [16] demonstrated data-driven prognostics of the PEMFC using a constraint based summation-wavelet extreme-learning machine algorithm.

Previous studies identified the early-stage degradation in the PEMFC system and provided information on its remaining useful life. Another model for estimating the degradation in PEMFCs has also been discussed in [5], [13]. This model uses an observer-based extended Kalman filter for estimating the state of health (SOH) and degradation of the PEMFC. The authors of [17] developed a prognostic algorithm based on a neural network paradigm. The degradation model discussed in [18] and [19] uses extreme-learning-machine and wavelet transforms for predicting the SOH. The authors of [19] proposed a data-fusion approach for forecasting the PEMFC performance based on long-short-term-memory, a recurrent neuron network, and the auto-regressive-integrated-moving-average method. The authors of [20] presented a complete empirical model of voltage degradation based on a linear function of the load profile. However, a simple linear load function may not be a good option for a complex PEMFC system. The aforementioned modelling approaches are complex and the models cannot be used for simultaneous fault diagnosis and prognostics because they cannot monitor the hydration state of the PEMFC. Besides, these models are used in signal processing, empirical formulas, control-based approaches, and artificial intelligence-based approaches. Although artificial intelligence-based approaches are accurate, their generalization to different types of PEMFC systems requires many modifications. In addition, these models are difficult to update due to their extra data requirements and complexity.

Similarly, the mechanistic model approach is complex because the electrochemical equations of the PEMFC are difficult to adopt for online purposes. In particular, they require a significant amount of extraneous information from the system and are computationally time intensive. Therefore, PEMFC systems are commonly modeled using semiempirical equations, [21]–[23], which are now used in fault diagnosis techniques and prognostics. The semiempirical equations of Zhou *et al.* [24] determine the age-variable parameters using suitable curve-fitting functions. Their model equations are extremely complex; however, simpler empirical equations were proposed for their future work. A simple semiempirical equation proposed by Jouin *et al.* [25] and Lu *et al.* [26] predicts the voltage degradation of the PEMFC. The model of Lu *et al.* [26] features semiempirical equations derived from the load current, the pressure of the fuel gases,

the temperature of the PEMFC, and the operating time. The voltage degradation in this model was accessed and validated, and the model can monitor the health of PEMFC systems online. However, the above-mentioned models cannot monitor and calculate the membrane water content during online monitoring. As noted by Naudy *et al.* [27], imbalance in the membrane water content is a major cause of PEMFC degradation. Naudy's study also revealed that the atmospheric temperature and relative humidity of the air majorly affect PEMFC degradation. A recent semiempirical model proposed by Khan *et al.* [28] considers the atmospheric conditions while embedding the calculations of the membrane water content. Their model is intended for flooding and drying fault diagnosis and has several inherent advantages (generic formulation, adaptability to different atmospheric conditions, and variable number of fuel cells in the stack). To handle extreme conditions (extremely high humidity, extreme heat, and/or aridity), the constant parameters of the model are presented in function form. In particular, the relative humidity of the air ( $RH_{air}$ ) and the ambient temperature ( $T_{amb}$ ) are provided as functions.

The model presented herein makes the following key contributions to the existing literature:

- (i) The voltage degradation is predicted from the PEMFC loading level and working hours (providing a prognostic feature).
- (ii) The accuracy improvement of the model is statistically analysed, and the time-dependent degradation of the voltage equations is included in the concentration voltage drop.
- (iii) Flooding and drying faults are easily diagnosed by comparing the membrane water content with threshold limits (providing a fault diagnosis feature).
- (iv) The model is less complex with less computational burden than the existing methods and is suitable for online purposes.

The voltage degradation and membrane water content in the proposed semiempirical model are primarily based on Lu *et al.* [26] and Khan *et al.* [28], respectively. The proposed model was first validated on a Horizon 500 W PEMFC. After upgrading and validating the Horizon 500 W PEMFC system, the parameters were optimized using a recently developed optimization technique known as the butterfly optimization algorithm (BOA) [29], in which variations in the parameters can be analyzed. The voltage degradation in the proposed model was compared with the experimental results in [24] under similar loading conditions. The model was updated in a statistical regression analysis using Minitab<sup>®</sup> software. The concentration voltage drop was updated using a new equation based on the time and loading current. With this equation, the voltage degradation output by the model matches that described by Zhou *et al.* [24]. The final proposed semiempirical model performs fault diagnosis, health monitoring, and estimation of the degradation voltage over long durations while working on the PEMFC. The membrane water content of the PEMFC system was calculated and

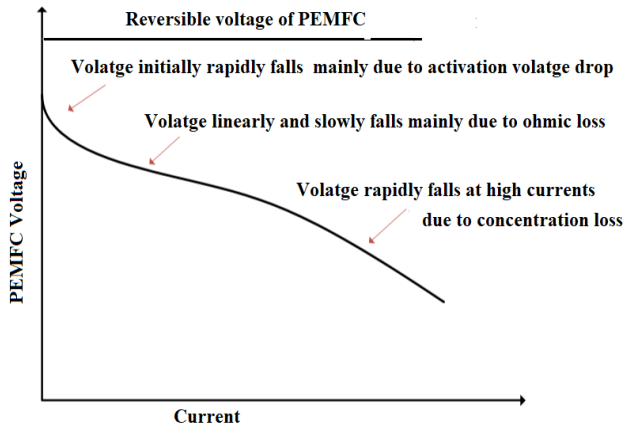


**FIGURE 1.** PEMFC nonlinear current-voltage characteristics.

simulated in Matlab<sup>®</sup>. The operating limits of the membrane water content were within the operating limits described by Khan *et al.* [28] (i.e., 7 to 11).

## II. GENERAL PEMFC VOLTAGE MODEL

The PEMFC voltage responds nonlinearly to a linear load change. It is described using complex electrochemical equations that primarily depend upon the temperature ( $T$ ) and geometry of the PEMFC, the pressure of the gases (i.e., hydrogen and oxygen ( $P_{H_2}$ ,  $P_{O_2}$ )), the load current ( $I$ ), and the number of fuel cells ( $N$ ) in a stack. The general equation of the PEMFC voltage is

$$V_{out} = E_{stack} - V_{act} - V_{ohm} - V_{con} \quad (1)$$

Here  $V_{out}$  and  $E_{stack}$  are the output voltage and electromagnetic field (EMF) of the PEMFC, respectively,  $V_{act}$  is the activation voltage drop,  $V_{ohm}$  is the ohmic voltage drop, and  $V_{con}$  is the concentration voltage drop. The current-voltage characteristic of the PEMFC is given in Figure 1.

### A. EMF OF STACK

The EMF of the stack is produced by a chemical reaction from the PEMFC as the hydrogen and oxygen atoms react in an exothermic reaction. The reaction produces electricity, water, and heat. The EMF is also called an irreversible open circuit voltage of the PEMFC. The produced EMF depends on the pressure of the fuel gases and the temperature of the PEMFC. The EMF of the PEMFC stack is calculated using the following Nernst equation:

$$EMF = N \left[ 1.229 - 8.5 \times 10^{-4} (T - 298) + \frac{RT}{2F} \left( \frac{P_{H_2} P_{O_2}^{0.5}}{P_{H_2O}} \right) \right] \quad (2)$$

Here,  $R$  is the gas constant ( $8.3143 \text{ J} \cdot \text{mol}^{-1} \text{ K}^{-1}$ ) and  $F$  is the Faraday constant ( $96,487 \text{ C} \cdot \text{mol}^{-1}$ ). The temperature  $T$  is expressed in Kelvin. The no-load voltage of the PEMFC stack is lower than the EMF of the stack because internal currents are generated by fuel gas crossover.

### B. ACTIVATION VOLTAGE DROP

The activation voltage was first observed by Dicks and Rand [11]. A drop in this voltage depends upon the reaction

speed and is given by Eq. (3). The over-voltage is not significant unless the load current ( $I$ ) exceeds the exchange current ( $I_o$ ).

$$V_{act} = A \log \left( \frac{I}{I_o} \right) \quad (3)$$

where the Tafel slope  $A$  measures the reaction speed and depends on the PEMF temperature. The exchange current depends on both the PEMFC temperature and the geometry of the PEMFC system. Different semiempirical models give different activation voltages depending on their load current and temperature function. After long-term operation, the activation voltage drops as the PEMFC ages. Zhou's model [24] reveals that the exchange current decreases over time.

### C. OHMIC VOLTAGE DROP

The ohmic voltage drop  $V_{ohm}$  of the PEMFC depends on the internal resistance of the PEMFC, which depends on the geometry of the PEMFC system (i.e., area of the fuel cell), the temperature ( $T$ ), and the loading current ( $I$ ). In general, the resistance of the PEMFC is divided into an ionic resistance ( $R_{ion}$ ) and an electronic resistance ( $R_e$ ). The ohmic resistance has been calculated by different formulas, but the ohmic voltage drop is fundamentally calculated by Ohm's law. Zhou *et al.* [24] also mentioned that the ohmic resistance increases over time, indicating that the ohmic voltage drop increases with aging effects.

### D. CONCENTRATION VOLTAGE DROP

The concentration voltage drops as the concentration of hydrogen decreases during the PEMFC operation. The concentration change reduces the partial pressure of the gases. The concentration reduction of the fuel gases depends on the electric current that is drawn. The concentration changes of the gases depend on the current, temperature, geometry of the electrodes, and the limiting current of the PEMFC ( $I_L$ ). The concentration voltage drop is calculated as

$$V_{con} = -B \left( 1 - \frac{I}{I_L} \right) \quad (4)$$

Here,  $B$  is the concentration voltage drop factor, which depends on the temperature of the PEMFC. The gases and limiting current [13]–[25] are also affected by the aging phenomena in the PEMFC system. Jouin *et al.* [25] revealed that the limiting current depends on the diffusion coefficient, which is negligibly impacted by age as demonstrated by Zhou *et al.* [24]. Therefore, the degradation effect of diffusion on the concentration voltage can be neglected.

## III. QLSA SEMIEMPIRICAL VOLTAGE MODEL OF PEMFC

The semiempirical model of Khan *et al.* [28] uses a quantum lightning search algorithm (QLSA) for optimization. The model equations start with the no-load voltage of the PEMFC, which is less than the EMF of the stack and is given by

$$V_{no-load} = N [1.229 - 8.5 \times 10^{-4} (T - 298) + \frac{RT}{2F} \ln (P_{H_2} P_{O_2}^{0.5}) - (V_{int} + V_{H_2O})] \quad (5)$$

As reported in two separate studies by Khan *et al.* [21], [28], the voltage drop ( $V_{int} + P_{H_2}$ ) is caused by the internal currents and the pressure of the water ( $P_{H_2O}$ ). The internal current is considered to be constant in a single cell,  $V_{H_2O}$  denotes the drop in the potential caused by  $P_{H_2O}$ , and  $V_{int}$  is the voltage induced by the internal current. One of the primary voltage drops is the activation voltage, expressed as

$$V_{act,1} = \frac{NRT}{2\alpha F} \ln\left(\frac{I}{I_o}\right) = \frac{RT}{2\frac{\alpha}{N}F} \ln\left(\frac{I}{I_o}\right) \text{ if } (I > I_o) \quad (6)$$

where  $I_o$  is represented as

$$I_o = B_1 \times F \times \exp\left(\frac{-1.229 \times B_2 \times F}{RT}\right) \quad (7)$$

The exchange current  $I_o$  in Eq. (7) is temperature-dependent and  $\alpha/N$  is the charge transfer coefficient, which measures the reaction speed. Parameters  $B_1$  and  $B_2$  depend on the symmetry of the PEMFC design.  $V_{ohm}$  refers to the voltage drop caused by the ohmic resistance of the PEMFC. The ionic resistance is more complex because it depends not only on the current and temperature of the PEMFC but also on the water content of the PEMFC membrane. The ionic resistance  $R_{ion}$  requires the pressure of the liquid water  $P_{H_2O}$  and the vapour pressure  $P_{vap}$ , which are calculated using Eqs. (8)–(10). In Eq. (8),  $NA_1$  and  $NA_2$  are constant parameters, which are optimized.

$$\begin{aligned} N \times V_{H_2O} &= NA_1 \times T \times P_{H_2} + NA_2 - N \times V_{int} \\ N \times (V_{H_2O} - V_{int}) &= N \times A_{H_2O} \times T \times \log(P_{H_2O}) \end{aligned} \quad (8)$$

$$P_{H_2O} = \exp\left(\frac{V_{H_2O}}{T \times A_{H_2O}}\right) \quad (9)$$

$$\begin{aligned} \log(P_{vap}) &= 6.02724 \times 10^{-3} + 4.38484 \times 10^{-4} (T - 273.15) \\ &+ 1.39844 \times 10^{-5} (T - 273.15)^2 \\ &+ 2.71166 \times 10^{-7} (T - 273.15)^3 \\ &+ 2.57731 \times 10^{-9} (T - 273.15)^4 \\ &+ 2.82254 \times 10^{-11} (T - 273.15)^5 \end{aligned} \quad (10)$$

Next, using the values of  $P_{H_2O}$  and  $P_{vap}$  calculated above, the relative humidity  $\varphi$  of the PEMFC is calculated as

$$\varphi = \frac{P_{H_2O}}{P_{vap}} \quad (11)$$

From the relative humidity  $\varphi$ , the water content of the membrane  $\lambda$  is determined as

$$\lambda = 0.043 + 17.81\varphi - 39.85\varphi^2 + 36\varphi^3 \quad (12)$$

$R_{ion}$  is then calculated using Eq. (13):

$$R_{ion} = C_1 \times 0.0022 \frac{\left[1 + 0.03I + 0.062\left(\frac{T}{303}\right)^2 I^{2.5}\right]}{(\lambda - 0.634 - 3I) \exp\left[4.18\left(\frac{T-303}{T}\right)\right]} \quad (13)$$

where the value of the constant  $C_1$  depends on the PEMFC membrane thickness. Note that  $C_1$  will vary with number

**TABLE 1. Parameters of the QLSA Semiempirical Model and Their Corresponding Symbols.**

Parameter description	Parameter symbol
Charge-transfer coefficient	$\alpha/N$
Exchange current coefficient	$B_1$
Exchange current density coefficient	$B_2$
Voltage drop due to internal current	$V_{int}$
Electronic resistance	$R_e$
Pressure of water constant	$A_{H_2O}$
Ionic resistance constant	$C_1$
First no-load voltage component	$NA_1$
Second no-load voltage component	$NA_2$

**TABLE 2. Parameter Functions When the Ambient Temperature and Relative Humidity Largely Deviate From Normal.**

Parameter	Parameter expressed as a function of ambient temperature ( $T_{amb}$ ) and relative air humidity ( $RH_{air}$ )
Charge-transfer coefficient ( $\alpha/N$ )	$\frac{\alpha}{N} = 0.007354 - 0.000084 \times T_{amb}$
Voltage drop due to the internal current ( $V_{int}$ )	$V_{int} = 0.253 - 0.00243T_{amb} - 0.000064T_{amb} \times RH_{air}$
Pressure of the water constant $A_{H_2O}$	$A_{H_2O} = 0.25333 - 0.002430T_{amb} - 0.000064T_{amb} \times RH_{air}$
$NA_1$	$NA_1 = 0.08529 - 0.001851T_{amb} - 0.000022T_{amb} \times RH_{air}$

Note: Here  $T_{amb}$  is in degrees Celsius and  $RH_{air}$  is a percentage.

of cells in the stack. Although  $R_e$  was supposed to be constant to reduce the computational complexity, it also varies with number of cells. Thus, the ohmic voltage drop  $V_{ohm}$  is expressed as

$$V_{ohm,1} = I (R_{ion} + R_e) \quad (14)$$

The last voltage drop, i.e., the concentration voltage drop  $V_{con}$ , is finally calculated by Eq. (15):

$$V_{con,1} = \frac{-NRT}{2F} \ln\left(1 - \frac{I}{I_{lim}}\right) \quad (15)$$

The parameters to be optimized and their symbols are listed in Table 1. The parameters vary in different PEMFCs, as mentioned by Khan *et al.* [28]. Some parameters can also be described as functions under abnormal ambient conditions (i.e., when the ambient temperature significantly varies from 298 K (25 °C) or the atmosphere is extremely dry or humid). The equations of the parameters are listed in Table 2 [28].

**TABLE 3. Parameter Di and Ei Values [26].**

Parameter	Value
$D_1$	$3.2725 \times 10^{-4}$
$D_2$	$1.6864 \times 10^{-6}$
$D_3$	$6.427 \times 10^{-4}$
$D_5$	$2.775 \times 10^{-8}$
$D_5$	$9.93 \times 10^{-4}$
$D_6$	0.709
$D_7$	127
$D_8$	0.00576
$D_9$	$1.78 \times 10^{-4}$
$E_1$	$7.013 \times 10^{-8}$
$E_2$	$4.656 \times 10^{-5}$
$E_3$	$8.188 \times 10^{-3}$
$E_4$	$2.508 \times 10^{-7}$

#### A. OPTIMIZING THE PARAMETERS WITH THE BUTTERFLY OPTIMIZATION ALGORITHM

A Horizon 500 W PEMFC was used in the experiments and the parameters were optimized using the butterfly optimization algorithm (BOA). The ambient changes were outside the study scope and all experiments were performed at 298 K, so the parameters were assigned constant values. The QLSA model has several advantages. First, it directly incorporates the ambient conditions and it can diagnose PEMFC flooding and drying faults. Second, it is suitable for monitoring the PEMFC hydration state online. It remains only to determine the degradation effects.

The model of Lu *et al.* [26] considers the voltage degradation over time by introducing a time variable  $t_h$  to the PEMFC voltage. The voltage drops  $V_{act,m}$  and  $V_{ohm,m}$  are respectively given by

$$V_{act,m} = \left\{ D_1 \times T + (-D_2 \times T + D_3 + D_4 \times t_h) \times T \right. \\ \left. \times \log \left( I + D_5 \times T^2 - D_6 \times T + D_7 + D_8 \times t_h \right) \right\} \\ + D_9 \times \log(P_{O_2}) \quad (16)$$

$$V_{ohm,m} = \left( E_1 \times T^2 - E_2 \times T + E_3 + E_4 \times t_h \right) \times I \quad (17)$$

The values of the parameters  $E_i$  and  $D_i$  are listed in Table 3.

The parameter  $t_h$  is given in hours. These parameters may also vary in the Horizon 500 W PEMFC. The parameters  $D_i$  were optimized using the BOA. The time-based term  $E_4 \times t_h$  in Eq. (17) can be added to Eq. (14), which computes  $V_{ohm}$ . However, the time-based terms  $D_4 \times t_h$  and  $D_8 \times t_h$  in Eq. (16) cannot be simply added to Eq. (6) (which computes  $V_{act}$ ) because  $D_8 \times t$  is in logarithmic form. Therefore, the parameters  $D_i$  in Eq. (16) need to be optimized. The exceptions were  $D_4$  and  $D_8$ , whose values in the NEXA 1.2 kW PEMFC system were set to those in the Horizon-500 W system. After extracting all parameters in Eq. (16) (except for  $D_4$  and  $D_8$ , which remained unchanged), Eq. (16) depicts the modified activation voltage  $V_{act,m}$  of the PEMFC system. In addition,

inserting  $E_4 \times t_h$  in Eq. (14) gives

$$V_{ohm,m1} = I (R_{ion} + R_e + E_4 \times t_h) \quad (18)$$

The modified output voltage  $V_{out,1}$  in the QLSA model is then given by

$$V_{out,1} = V_{no-load} - V_{act,m} - V_{ohm,m1} - V_{con,1} \quad (19)$$

The time-based parameters  $E_4$ ,  $D_4$ , and  $D_8$  were assumed constant because these parameters probably do not depend on the PEMFC system. Rather, they depend on the working duration of the PEMFC. The modified QLSA model enables monitoring of the membrane water content  $\lambda$ ; the equations of  $R_{ion}$  will not change.

#### IV. BUTTERFLY OPTIMIZATION ALGORITHM (BOA)

Arora and Singh [29] recently discussed a novel optimization technique that mimics the behavior of butterflies searching for food and a mating partner. The BOA provides better and more efficient results than other optimization algorithms such as the genetic algorithm, cuckoo search, monarch butterfly optimization, and particle swarm optimization.

Butterflies have extremely sharp senses for seeking mating partners and food. These strong senses primarily explain their survival for over a million years. Butterflies' sense of smell is particularly important. Butterflies are attracted to the fragrance of a flower, which is unique to a flower species. In the BOA, the fragrance  $f$  depends on the physical stimulus  $I_s$  and a parameter  $a$  called the power exponent. The parameter  $a$  allows for a linear response, regular compression, and expansion. The fragrance is calculated as

$$f = c I_s^a \quad (20)$$

where  $c$  is the sensory modality and the values of  $a$  and  $c$  are within the range  $[0, 1]$ . If  $a$  is unity, the fragrance is fully absorbed by other butterflies, meaning that the fragrance is emitted in an ideal environment. Conversely, when  $a$  is zero, the fragrance emitted cannot be sensed by other butterflies. The parameter  $c$  is crucial because it determines the speed of convergence. The stimulus  $I_s$  is based on the objective function of the system to be optimized, which is the root mean square. In this work,  $V_{exp}$  is the experimentally determined voltage of the PEMFC. The root mean square error (RMSE) is calculated as

$$RMSE = \sqrt{\frac{\sum (V_{out,1} - V_{exp})^2}{\text{Total number of samples}}} \quad (21)$$

Butterfly movements are influenced by the following factors:

- (i) The fragrance emitted by the butterflies, which attracts other butterflies.
- (ii) Every butterfly moves randomly or toward the butterfly emitting the most fragrance.
- (iii) The objective function, which determines the stimulus intensity  $I_s$  of a butterfly.

Optimization is a three-phase process of initialization, iteration, and finalization. In each run, the parameters are initialized. The initial population of the butterflies is set and

TABLE 4. Implementation of the BOA Algorithm.

Butterfly optimization algorithm (BOA)
Objective function RMSE(parameters), dim = no. of dimensions/parameters
Generate initial population of butterflies
Calculate the stimulus intensity $I_s$ using the RMSE function (Eq. (21))
Define parameters $c$ and $a$ and the switch probability $p$
<b>While</b> stopping criteria not met <b>do</b>
<b>For</b> each butterfly in the population <b>do</b>
Calculate fragrance for each butterfly using Eq. (20)
<b>End For</b>
Find the best butterfly
<b>For</b> each butterfly in the population <b>do</b>
Generate a random number $r$
<b>If</b> $r < p$ , <b>then</b>
Move towards the best butterfly using Eq. (22)
<b>Else</b>
Move randomly using Eq. (23)
<b>End if</b>
<b>End for</b>
Update the value of $a$
<b>End While</b>
Output best solution

their positions are randomly generated in the search space (i.e., the given ranges, fragrance, and fitness values are calculated and stored).

Subsequently, during each iteration, all butterflies move to a new position and their fitness values and fragrances are calculated by Eqs. (20) and (21), respectively. The search phase has two main steps: global search and local search.

During the global search, the movement is biased toward the fittest butterfly, as shown in Eq. (22):

$$x_{i,t+1} = x_{i,t} + \left( r^2 \times g^* - x_{i,t} \right) \times f_i \quad (22)$$

Here,  $x_{i,t}$  is the solution vector of the  $i$ th butterfly in iteration  $t$ ,  $g^*$  is the current best solution in the current iteration, and  $f_i$  is the fragrance of the  $i$ th butterfly.  $r$  is a random number between 0 and 1 inclusive.

The local search phase of the butterflies is governed by Eq. (23):

$$x_{i,t+1} = x_{i,t} + \left( r^2 \times x_{j,t} - x_{i,t} \right) \times f_i \quad (23)$$

Here,  $x_{i,t}$  and  $x_{j,t}$  are the  $i$ th and  $j$ th butterflies in the solution space, respectively. If  $x_{i,t}$  and  $x_{j,t}$  belong to the same swarm, Eq. (23) describes a local random walk.

The last phase of the algorithm is terminated when the best solution is found or when the maximum number of iterations is achieved. In this study, the stopping criterion was the maximum number of iterations. The basic structure of the BOA is given in Table 4. The algorithm uses a switch probability factor  $p$  which changes the search phase from a global to a local search.

### V. EXPERIMENTS

Experiments were performed on the Horizon-500 W PEMFC system, which has 36 fuel cells in the stack and a limiting current ( $I_L$ ) of 42 A. The experimental setup consisted of a pressure regulator, a DC electronic load, and a controller for the PEMFC system.

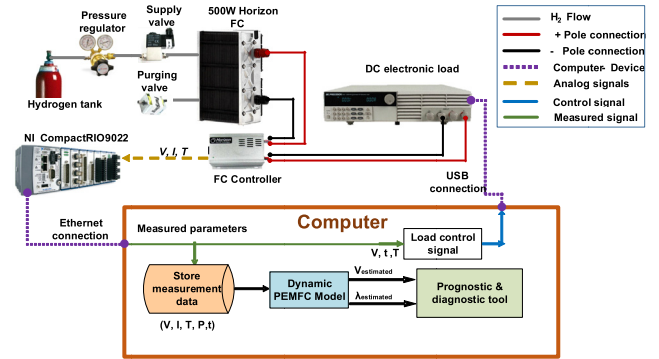


FIGURE 2. Experimental setup of the Horizon 500-W PEMFC system.

Figure 2 is a schematic of the complete PEMFC system [1]. The experiments were performed for 3232 s (0.89 hr) at  $T_{amb} = 25^\circ\text{C}$  (298 K). The load current was varied haphazardly and the hydrogen pressure ( $P_{H_2}$ ) was constantly maintained at 0.55 atm. The air pressure was assumed to be constant at 1 atm. The samples were obtained after 0.1 s. The time courses of the voltage  $V_{exp}$ , current  $I$ , and temperature  $T$  of the PEMFC are presented in Figure 3.

The ranges of the final optimized parameters are given in Table 5.

### VI. RESULTS AND DISCUSSION

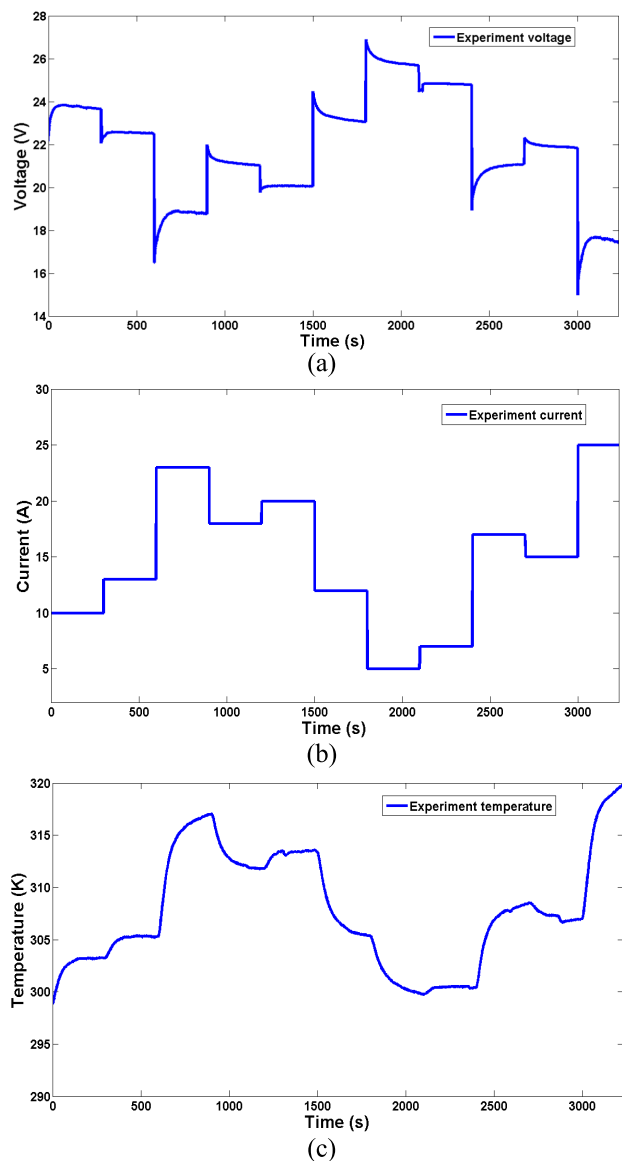
Parameter optimization is the first primary step toward obtaining the results. After 600 iterations, the optimization results were deemed sufficient because the RMSE was below 0.5 for a sample size of approximately 32,000.

Figure 4 shows the optimization progress and a comparison between the modeled and experimental voltages. The final values of the parameters are provided in Table 6.

The term  $\alpha/N$  exerted the lowest impact and was independent of the air relative humidity ( $RH_{air}$ ). Therefore, neglecting  $\alpha/N$  will negligibly affect the model's output under the loading conditions.

The working period of the PEMFC has not been tested. Here, the voltage variations over  $t_h$  were observed under different load currents. The voltage effects over 400 hours were first simulated under low currents. At 5 A (almost 11% of the limiting current), the recorded temperature was 299.52 K and the experimental voltage was 25.29 V. The hydrogen pressure remained constant at 0.55 atm and the air pressure was 1 atm. Zhou et al. [24] tested another PEMFC system for 400 hours under a similar current. In the present study, the voltage decreased by approximately 1.0 V over the 400-hour observation period.

Figure 5 shows the voltage variations over  $t_h$  under a low current. In the model simulations, the voltage varied by approximately 1.0 V. The degradation of the PEMFC voltage was tested at 17 A (almost 40% of the limiting current), where the PEMFC temperature was 308.93 K and the experimental voltage was 21.06 V. The fuel gas pressures were those at 5 A. Zhou et al. [24] monitored the voltage



**FIGURE 3.** Experimental results of the Horizon 500 PEMFC: (a) voltage, (b) current, and (c) temperature.

degradation for 400 hours at 17 A, and reported a drop of approximately 2.25 V. However, in Figure 6, the drop was only approximately 0.5 V.

Finally, the degradation of the PEMFC was tested at 25 A (almost 60% of the limiting current). The temperature and experimental voltage were 319.84 K and 17.8 V, respectively. At a similar current, Zhou *et al.* [24] reported a voltage degradation of slightly above 3.7 V after 400 hours. However, Figure 7 reveals a voltage degradation of just under 0.5 V after 400 hours in the proposed model.

Voltage degradation has many causes, as mentioned in the Introduction. Therefore, a PEMFC cannot sustain its output over 400 h of operation. The model presented by Zhou *et al.* [24] applied the particle filter approach, which introduces some obvious errors when fitting to the experimental results.

**TABLE 5.** BOA-Optimized Parameter Ranges in the Proposed Semiempirical Model.

Parameter	Lower Range	Upper Range
$D_1$	$1 \times 10^{-5}$	$1 \times 10^{-2}$
$D_2$	$1 \times 10^{-7}$	$1 \times 10^{-3}$
$D_3$	$1 \times 10^{-5}$	$1 \times 10^{-2}$
$D_5$	$1 \times 10^{-4}$	$2 \times 10^{-3}$
$D_6$	$1 \times 10^{-1}$	1.4
$D_7$	100	150
$C_1$	$1 \times 10^{-1}$	2
$D_9$	$1 \times 10^{-5}$	$1 \times 10^{-1}$
$R_e$	$1 \times 10^{-2}$	$1 \times 10^{-1}$
$A_{H_2,0}$	$1 \times 10^{-2}$	1
$NA_1$	$1 \times 10^{-3}$	1
$V_{int}$	$1 \times 10^{-2}$	$5 \times 10^{-1}$
$NA_2$	$1 \times 10^{-1}$	30

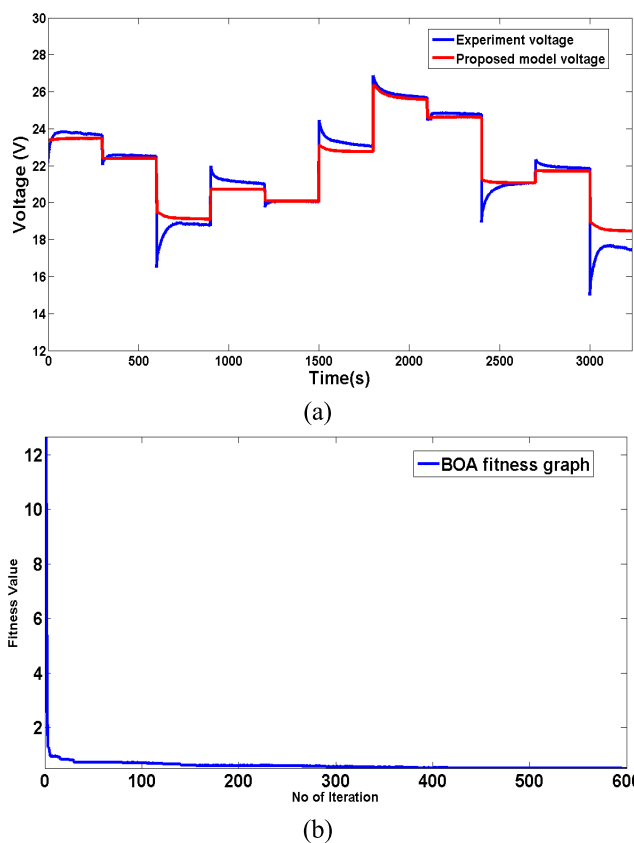


**FIGURE 4.** (a) Comparison of the experimental and modeled voltages in the Horizon 500-W PEMFC, and (b) fitness optimization by BOA.

**A. STATISTICAL REGRESSION ANALYSIS**

The voltage degradation results at high current deviated from the experimental results of Zhou *et al.* [24], as highlighted in Table 7.

To improve the model, we performed statistical regression analysis with the  $t_h$  and percentage current ( $I_p$ ) as the main covariates (see Table 8). For low currents (i.e., 5A (~11% of the limiting current)), the results were satisfactory; however, the approach failed at higher currents (i.e., 17 A (40%) and 25 A (60%)).

TABLE 6. Final Parameter Values After BOA Optimization.

Parameter	Final Value
$D_1$	$9.99 \times 10^{-3}$
$D_2$	$4.26 \times 10^{-7}$
$D_3$	$1 \times 10^{-2}$
$D_5$	$1 \times 10^{-4}$
$D_6$	$4.77 \times 10^{-1}$
$D_7$	135.7913
$C_1$	$4.99 \times 10^{-1}$
$D_9$	$1.0032 \times 10^{-5}$
$R_e$	$9.3899 \times 10^{-2}$
$A_{H_2O}$	$1.4985 \times 10^{-1}$
$NA_1$	$3.965 \times 10^{-2}$
$V_{int}$	$1.498499 \times 10^{-1}$
$NA_2$	1.88223

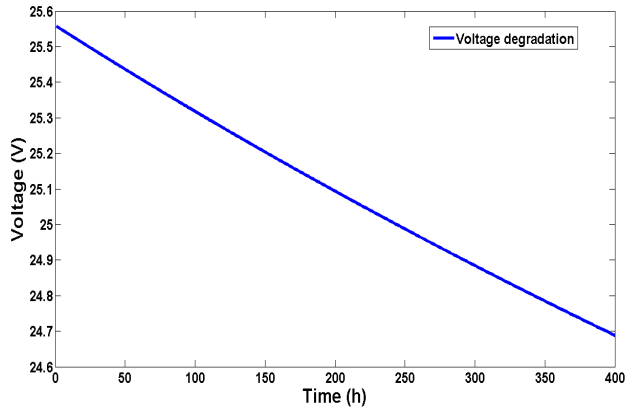


FIGURE 5. Voltage monitored for 400 hours at 5 A ( $T = 299.52$  K).

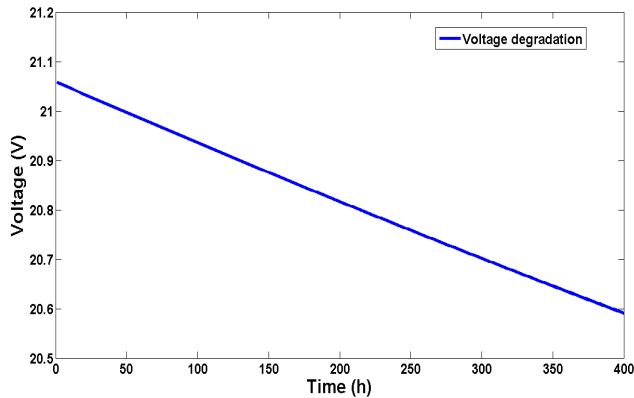


FIGURE 6. Voltage degradation in theHorizon 500-W simulate for 400 hours at 17 A ( $T = 308.93$  K).

The voltage differences  $V_d$  between the experimentally determined voltage degradation (described by Zhou *et al.* [24]) and that determined using the proposed model were determined at 100, 200, 300, and 400 h for different output current percentages ( $I_p$ ) (40% and 60%). The residual plot and results of the normality test are shown in Figure 8. The residuals were normal because the p-value exceeded 0.05.

The final regression equation of  $V_d$  is given by Eq. (24). The effects of  $t_h$  and  $I_p$  were insignificant ( $p > 0.05$ );

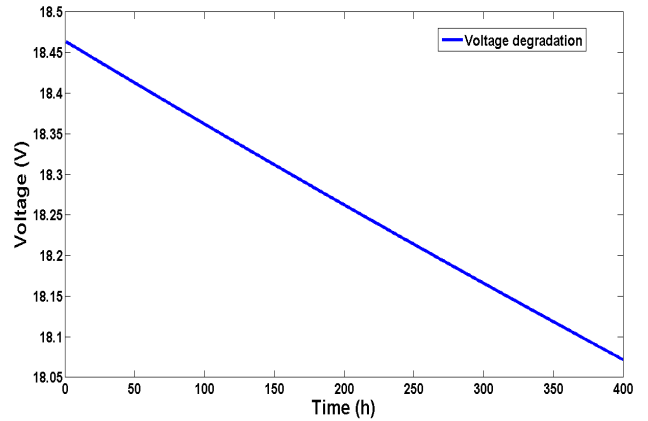


FIGURE 7. Voltage degradation in theHorizon 500-W voltage degradation simulated for 400 hours at 25 A ( $T = 319.84$  K).

TABLE 7. Comparison of Voltage Degradations Obtained Using the BOA-Optimized Proposed Model and the Approximate Experimental Results of ZHOU [24].

Current Percentage w.r.t to the maximum current % ( $I_p$ )	Time (Hours)	Temperature (K)	Experimental voltage degradation on $V_1$ [24]	Modeled voltage degradation on $V_2$	$V_d = V_1 - V_2$
40	1	308.93	0.002	0.001	0.001
40	100	308.93	0.25	0.1149	0.1351
40	200	308.93	0.5	0.2308	0.2692
40	300	308.93	1.6	0.3428	1.2572
40	400	308.93	2.25	0.4512	1.7988
60	1	319.84	0.002	0.001	0.001
60	100	319.84	0.25	0.1012	0.1488
60	200	319.84	0.6	0.2006	0.3994
60	300	319.84	2.6	0.2972	2.3028
60	400	319.84	3.7	0.3913	3.3087

TABLE 8. Analysis of Variance of the Transformed Response (Using the Current and Working Hours of the PEMFC as Covariates).

Source	DF	Adj SS	Adj MS	F - Value	P - Value
$t_h$	1	0.5968	0.59681	5.64	0.063
$I_p$	1	0.0621	0.06206	0.59	0.478
$t_h^2$	1	0.8960	0.89596	8.47	0.033
$t_h \times I_p$	1	0.8219	0.82191	7.77	0.039
Error	5	0.5286	0.10573		
Total	9	12.0807			
Model Summary					
S	R-sq	R-sq(adj)	R-sq(pred)		
0.325158	95.62%	92.12%	81.74%		

however, the squared  $t_h$  term and its interactions were significant. The hierarchy of the statistical regression design  $t_h$ , and  $I_p$  must also be included:

$$V_d = \begin{cases} 0.657 - 0.0137I_p + 0.000018t_h^2 \\ \quad + 0.000203t_hI_p \text{ for } I_p > 30\% \\ 0 \text{ for } I_p < 30\% \end{cases} \quad (24)$$

As the previous time-based degradation was not applied to the concentration voltage, it was assumed that when the current percentage ( $I_p$ ) reached 30%, the voltage degradation of  $V_{ohm}$

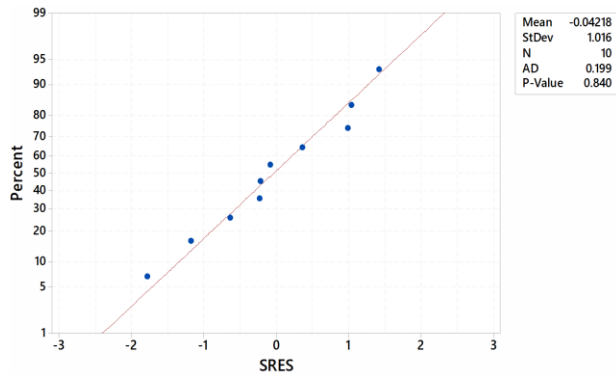


FIGURE 8. Residual plot and results of normality test.

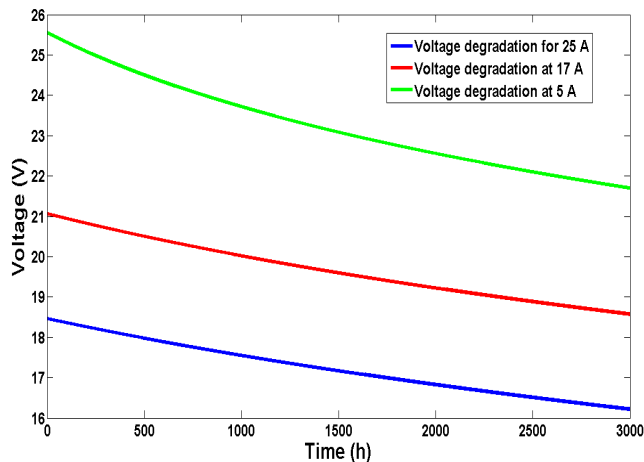


FIGURE 9. Comparison of voltage degradations at different currents.

and  $V_{act}$  alone could not explain the observed degradation. Therefore,  $V_d$  was added to  $V_{con,1}$ , the time-based voltage drop term for the concentration voltage. Bressel *et al.* [5] also revealed that a time-based degradation term is necessary for the concentration voltage.

The new concentration voltage  $V_{con,2}$  was determined as follows:

$$V_{con,2} = \frac{-NRT}{2F} \ln \left( 1 - \frac{I}{I_{lim}} \right) + V_d \quad (25)$$

Figure 9 compares the voltage degradations at 5, 17, and 25 A using  $V_d$  in the proposed model. The results were more satisfactory than the previous results at high currents (c.f. Figure 9 and Figures 6 and 7).

### B. MEMBRANE WATER CONTENT FOR FAULT DIAGNOSIS

The proposed model can diagnose flooding and drying faults. The present experiment was performed under normal conditions, when no flooding and drying faults can occur. Khan *et al.* [28] suggested that the normal range of membrane water contents  $\lambda$  is 7–11. The time-varying membrane water content  $\lambda$  of the proposed model is plotted in Figure 10. The experimental results in Figure 3 confirm that the membrane water content remained within normal limits; hence, the proposed model can diagnose faults with sufficient accuracy.

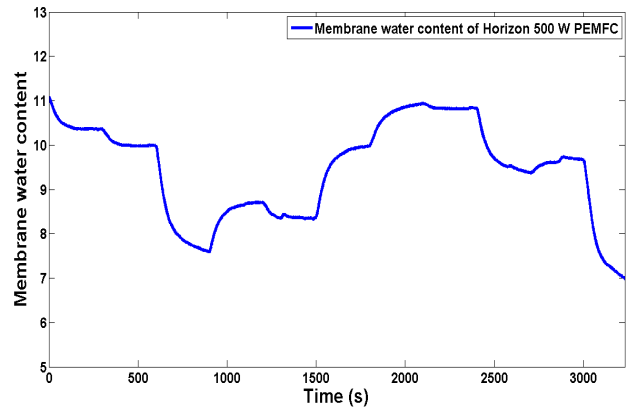


FIGURE 10. Membrane water content in the Horizon 500 W PEMFC.

If the membrane water content is below 7, the membrane is excessively dry, and if it exceeds 11, a flooding fault has occurred. Based on the techniques in [30] and [31], smart and intelligent techniques for other PEMFC fault diagnoses must be explored in future.

### VII. CONCLUSION

This study proposed a semiempirical model with modified activation, ohmic, and concentration voltage drops reflecting the performance deterioration over time (hours). The novel component of this work is the proposed concentration voltage drop, which was calculated through a statistical regression analysis. In the simulation study, the results of the proposed voltage degradation model were apparently consistent with the experimental degradation reported in the literature. In particular, the degradation in PEMFC voltage was discussed at different load currents. The proposed semiempirical model is useful for both fault diagnosis and prognostics, and is especially advantageous for online monitoring and abnormal diagnoses of membrane water content. The equations are relatively simple and computationally time-efficient. Degradation is caused by many factors and the PEMFC experiences many transients during long-term operation. Nevertheless, the degradation estimation model is a useful tool for operators. The present model estimates the degradation in PEMFCs operating under normal ambient conditions, but the model parameters can be modified for abnormal ambient conditions by incorporating the equations developed herein. In future work, the model will be checked and validated for the prognosis and diagnosis of other types of PEMFC systems. Incorporating the area and membrane thickness of the PEMFC will generalize the parameters and realize a more generic model. After some modifications, a model that is applicable to most PEMFC systems without requiring any optimization techniques is expected to become available in future.

### ACKNOWLEDGMENT

The authors would like to thank UAEU library and Mr. Shehab Majud for the spell check and valuable proof-reading. They would also like to thank UAEU for Open Access Publishing.

## REFERENCES

- [1] M. Kandidayeni, A. Macias, A. Khalatbarisoltani, L. Boulon, and S. Kelouani, "Benchmark of proton exchange membrane fuel cell parameters extraction with metaheuristic optimization algorithms," *Energy*, vol. 183, pp. 912–925, Sep. 2019, doi: [10.1016/j.energy.2019.06.152](https://doi.org/10.1016/j.energy.2019.06.152).
- [2] S. S. Khan, H. Shareef, and A. H. Mutlag, "Dynamic temperature model for proton exchange membrane fuel cell using online variations in load current and ambient temperature," *Int. J. Green Energy*, vol. 16, no. 5, pp. 361–370, Apr. 2019, doi: [10.1080/15435075.2018.1564141](https://doi.org/10.1080/15435075.2018.1564141).
- [3] S. S. Khan, H. Shareef, A. Wahyudie, S. Khalid, and R. Sirjani, "Influences of ambient conditions on the performance of proton exchange membrane fuel cell using various models," *Energy Environ.*, vol. 30, no. 6, pp. 1087–1110, Sep. 2019, doi: [10.1177/0958305X18802775](https://doi.org/10.1177/0958305X18802775).
- [4] M. Jourdan, H. Mounir, and A. El Marjani, "Compilation of factors affecting durability of proton exchange membrane fuel cell (PEMFC)," in *Proc. Int. Renew. Sustain. Energy Conf. (IRSEC)*, Ouarzazate, Morocco, Oct. 2014, pp. 542–547, doi: [10.1109/IRSEC.2014.7059906](https://doi.org/10.1109/IRSEC.2014.7059906).
- [5] M. Bressel, M. Hilairat, D. Hissel, and B. O. Bouamama, "Remaining useful life prediction and uncertainty quantification of proton exchange membrane fuel cell under variable load," *IEEE Trans. Ind. Electron.*, vol. 63, no. 4, pp. 2569–2577, Apr. 2016, doi: [10.1109/TIE.2016.2519328](https://doi.org/10.1109/TIE.2016.2519328).
- [6] M. Chandesris, R. Vincent, L. Guetaz, J.-S. Roch, D. Thoby, and M. Quinaud, "Membrane degradation in PEM fuel cells: From experimental results to semi-empirical degradation laws," *Int. J. Hydrogen Energy*, vol. 42, no. 12, pp. 8139–8149, Mar. 2017, doi: [10.1016/j.ijhydene.2017.02.116](https://doi.org/10.1016/j.ijhydene.2017.02.116).
- [7] K. A. El, L. Flandin, and C. Bas, "Chemical degradation of PFSA ionomer binder in PEMFC's catalyst layer," *Int. J. Hydrogen Energy*, vol. 43, no. 32, pp. 1539–15386, 2018, doi: [10.1016/j.ijhydene.2018.06.049](https://doi.org/10.1016/j.ijhydene.2018.06.049).
- [8] L. Cindrella, A. M. Kannan, J. F. Lin, K. Saminathan, Y. Ho, C. W. Lin, and J. Wertz, "Gas diffusion layer for proton exchange membrane fuel cells—A review," *J. Power Sources*, vol. 194, no. 1, pp. 146–160, Oct. 2009, doi: [10.1016/j.jpowsour.2009.04.005](https://doi.org/10.1016/j.jpowsour.2009.04.005).
- [9] J. Wind, R. Späh, W. Kaiser, and G. Böhm, "Metallic bipolar plates for PEM fuel cells," *J. Power Sources*, vol. 105, no. 2, pp. 256–260, 2002, doi: [10.1016/S0378-7753\(01\)00950-8](https://doi.org/10.1016/S0378-7753(01)00950-8).
- [10] B. G. Pollet, I. Staffell, and J. L. Shang, "Current status of hybrid, battery and fuel cell electric vehicles: From electrochemistry to market prospects," *Electrochim. Acta*, vol. 84, pp. 235–249, Dec. 2012, doi: [10.1016/j.electacta.2012.03.172](https://doi.org/10.1016/j.electacta.2012.03.172).
- [11] A. Dicks and D. Rand, *Fuel Cell Systems Explained*, 3rd ed. Hoboken, NJ, USA: Wiley, 2018.
- [12] W. Li and A. M. Lane, "Analysis of oxygen sources and reaction pathways of carbon support corrosion at the cathode in PEMFC using oxygen-18 DEMS," *Electrochim. Acta*, vol. 55, no. 22, pp. 6926–6931, Sep. 2010, doi: [10.1016/j.electacta.2010.04.105](https://doi.org/10.1016/j.electacta.2010.04.105).
- [13] M. Bressel, M. Hilairat, H. Daniel, and B. Bouamama, "Aging tolerant control of proton exchange membrane fuel cell: A model-based approach," in *Proc. Conf. Adv. Control Diagnosis (ACD)*, Bucarest, Romania, Nov. 2017, pp. 1–7.
- [14] L. Elodie, G. Rafael, P. Marie-Cécile, H. Daniel, and Z. Noureddine, "Towards an ageing model of a PEMFC for prognostics purpose," in *Proc. Int. Discuss. Hydrogen Energy Appl.*, Nantes, France, Nov. 2016, pp. 1–7.
- [15] E. Lechartier, R. Gouriveau, M.-C. Pera, D. Hissel, and N. Zerhouni, "Static and dynamic modeling of a PEMFC for prognostics purpose," in *Proc. IEEE Vehicle Power Propuls. Conf. (VPPC)*, Coimbra, Portugal, Oct. 2014, pp. 1–5, doi: [10.1109/VPPC.2014.7007136](https://doi.org/10.1109/VPPC.2014.7007136).
- [16] K. Javed, R. Gouriveau, N. Zerhouni, and D. Hissel, "Improving accuracy of long-term prognostics of PEMFC stack to estimate remaining useful life," in *Proc. IEEE Int. Conf. Ind. Technol. (ICIT)*, Seville, Spain, Mar. 2015, pp. 1047–1052, doi: [10.1109/ICIT.2015.7125235](https://doi.org/10.1109/ICIT.2015.7125235).
- [17] S. Morando, S. Jemei, D. Hissel, R. Gouriveau, and N. Zerhouni, "Proton exchange membrane fuel cell ageing forecasting algorithm based on echo state network," *Int. J. Hydrogen Energy*, vol. 42, no. 2, pp. 1472–1480, Jan. 2017, doi: [10.1016/j.ijhydene.2016.05.286](https://doi.org/10.1016/j.ijhydene.2016.05.286).
- [18] K. Chen, S. Laghrouche, and A. Djerdir, "Degradation model of proton exchange membrane fuel cell based on a novel hybrid method," *Appl. Energy*, vol. 252, Oct. 2019, Art. no. 113439, doi: [10.1016/j.apenergy.2019.113439](https://doi.org/10.1016/j.apenergy.2019.113439).
- [19] R. Ma, Z. Li, E. Breaz, C. Liu, H. Bai, P. Briois, and F. Gao, "Data-fusion prognostics of proton exchange membrane fuel cell degradation," *IEEE Trans. Ind. Appl.*, vol. 55, no. 4, pp. 4321–4331, Jul. 2019, doi: [10.1109/TIA.2019.2911846](https://doi.org/10.1109/TIA.2019.2911846).
- [20] X. Zhang, D. Yang, M. Luo, and Z. Dong, "Load profile based empirical model for the lifetime prediction of an automotive PEM fuel cell," *Int. J. Hydrogen Energy*, vol. 42, no. 16, pp. 11868–11878, Apr. 2017, doi: [10.1016/j.ijhydene.2017.02.146](https://doi.org/10.1016/j.ijhydene.2017.02.146).
- [21] S. S. Khan, H. Shareef, A. Wahyudie, and S. N. Khalid, "Novel dynamic semiempirical proton exchange membrane fuel cell model incorporating component voltages," *Int. J. Energy Res.*, vol. 42, no. 8, pp. 2615–2630, Jun. 2018, doi: [10.1002/er.4038](https://doi.org/10.1002/er.4038).
- [22] R. Salim, M. Nabag, H. Noura, and A. Fardoun, "The parameter identification of the nexa 1.2 kW PEMFC's model using particle swarm optimization," *Renew. Energy*, vol. 82, pp. 26–34, Oct. 2015, doi: [10.1016/j.renene.2014.10.012](https://doi.org/10.1016/j.renene.2014.10.012).
- [23] S. S. Khan, H. Shareef, I. A. Khan, V. Bhattacharjee, and K. W. Sultan, "Effect of ambient conditions on water management and faults in PEMFC systems: A review," in *Proc. IEEE Can. Conf. Electr. Comput. Eng. (CCECE)*, Edmonton, AB, Canada, May 2019, pp. 1–5, doi: [10.1109/CCECE.2019.8861579](https://doi.org/10.1109/CCECE.2019.8861579).
- [24] D. Zhou, Y. Wu, F. Gao, E. Breaz, A. Ravey, and A. Miraoui, "Degradation prediction of PEM fuel cell stack based on multiphysical aging model with particle filter approach," *IEEE Trans. Ind. Appl.*, vol. 53, no. 4, pp. 4041–4052, Jul. 2017, doi: [10.1109/TIA.2017.2680406](https://doi.org/10.1109/TIA.2017.2680406).
- [25] M. Jouin, R. Gouriveau, D. Hissel, M.-C. Péra, and N. Zerhouni, "Degradations analysis and aging modeling for health assessment and prognostics of PEMFC," *Rel. Eng. Syst. Saf.*, vol. 148, pp. 78–95, Apr. 2016, doi: [10.1016/j.res.2015.12.003](https://doi.org/10.1016/j.res.2015.12.003).
- [26] L. Lu, M. Ouyang, H. Huang, P. Pei, and F. Yang, "A semi-empirical voltage degradation model for a low-pressure proton exchange membrane fuel cell stack under bus city driving cycles," *J. Power Sources*, vol. 164, no. 1, pp. 306–314, Jan. 2007, doi: [10.1016/j.jpowsour.2006.10.061](https://doi.org/10.1016/j.jpowsour.2006.10.061).
- [27] S. Naudy, F. Collette, F. Thominet, G. Gebel, and E. Espuche, "Influence of hydrothermal aging on the gas and water transport properties of Nafion membranes," *J. Membrane Sci.*, vol. 451, pp. 293–304, Feb. 2014, doi: [10.1016/j.memsci.2013.10.013](https://doi.org/10.1016/j.memsci.2013.10.013).
- [28] S. S. Khan, H. Shareef, C. Bouhaddioui, and R. Errouissi, "Membrane-hydration-state detection in proton exchange membrane fuel cells using improved ambient-condition-based dynamic model," *Int. J. Energy Res.*, vol. 44, no. 2, pp. 869–889, 2020, doi: [10.1002/er.4927](https://doi.org/10.1002/er.4927).
- [29] S. Arora and S. Singh, "Butterfly optimization algorithm: A novel approach for global optimization," *Soft Comput.*, vol. 23, no. 3, pp. 715–734, Feb. 2019, doi: [10.1007/s00500-018-3102-4](https://doi.org/10.1007/s00500-018-3102-4).
- [30] J. Long, S. Zhang, and C. Li, "Evolving deep echo state networks for intelligent fault diagnosis," *IEEE Trans. Ind. Informat.*, vol. 16, no. 7, pp. 4928–4937, Jul. 2020, doi: [10.1109/TII.2019.2938884](https://doi.org/10.1109/TII.2019.2938884).
- [31] J. Long, J. Mou, L. Zhang, S. Zhang, and C. Li, "Attitude data-based deep hybrid learning architecture for intelligent fault diagnosis of multi-joint industrial robots," *J. Manuf. Syst.*, to be published, doi: [10.1016/j.jmsy.2020.08.010](https://doi.org/10.1016/j.jmsy.2020.08.010).



**SAAD SALEEM KHAN** received the B.S. and M.S. degrees in electrical engineering power from the University of Engineering and Technology Lahore, Pakistan, and the Ph.D. degree from United Arab Emirates University, United Arab Emirates, in 2019. He is currently a part-time Post-doctoral Researcher with United Arab Emirates University, and also an Assistant Manager Technical with National Transmission and Despatch Company Limited, Pakistan. He is also doing research on modeling and fault diagnosis of fuel cell.



**HUSSAIN SHAREEF** (Member, IEEE) received the B.Sc. degree (Hons.) from IIT Dhaka, Dhaka, Bangladesh, in 1999, the M.S. degree from METU, Turkey, in 2002, and the Ph.D. degree from UTM, Malaysia, in 2007. He is currently a Professor with the Department of Electrical Engineering, United Arab Emirates University. His current research interests include power system optimization, power quality, artificial intelligence, renewable energy systems, and power system automation.



**MOHSEN KANDIDAYENI** (Member, IEEE) was born in Tehran, Iran, in 1989. He received the B.S. degree in mechanical engineering and the master's degree in mechatronics from Arak University, Iran, in 2011 and 2014, respectively, and the Ph.D. degree in electrical engineering from the University of Quebec, in 2020. In 2016, he joined the Hydrogen Research Institute, Université du Québec à Trois-Rivières, Trois-Rivières, QC, Canada. He was a straight-A student during

his master's and Ph.D. programs and a recipient of a doctoral scholarship from the Fonds de recherche du Québec–Nature et technologies (FRQNT). His research interests include energy-related topics such as hybrid electric vehicles, fuel cell systems, energy management, multiphysics systems, modeling, and control.



**LOÏC BOULON** (Senior Member, IEEE) received the master's degree in electrical and automatic control engineering from the University of Lille, France, in 2006, and the Ph.D. degree in electrical engineering from the University of Franche-Comté, France. Since 2010, he has been a Professor with the Université du Québec à Trois-Rivières (UQTR). Since 2016, he has been a Full Professor with the Hydrogen Research Institute. His work deals with modeling, control, and energy manage-

ment of multiphysics systems. He has published more than 120 scientific articles in peer-reviewed international journals and international conferences and given more than 35 invited conferences all over the world. His research interests include hybrid electric vehicles, energy and power sources (fuel cell systems, batteries, and ultracapacitors). Since 2019, he has been the world most cited authors of the topic “Proton Exchange Membrane Fuel Cells (PEMFC); Fuel Cells; Cell Stack,” Elsevier SciVal. In 2015, he was a General Chair of the IEEE Vehicular Power and Propulsion Conference, Montreal, QC, Canada. He is currently VP-Motor Vehicles of the IEEE Vehicular Technology Society. He found the International Summer School on Energetic Efficiency of Connected Vehicles and the IEEE VTS Motor Vehicle Challenge. He is the Holder of the Canada Research Chair in Energy Sources for the Vehicles of the future.



**ABBOU AMINE** was born in Oujda, Morocco. He received the Baccalaureate degree in mathematics and the Engineering Diploma degree in renewable energy and electro mechanics from the Higher National School of Mines of Rabat, Morocco, in 2006 and 2013, respectively, and the Ph.D. degree in engineering from the Smart & Sustainable Systems Research Department, Mohammadia School of Engineering, Rabat, Morocco. His current research interests include fuel cells as

a solution of storage of energy (more exactly, developing new methods for modeling and control of fuel cells).



**EL HASNAOUI ABDENNEBI** received the Ph.D. degree in sciences and applications from the Université de Toulouse, France, in 1987. He is currently the Head of the Electro Mechanics Department, Superior School of Mines, Rabat, Morocco, and also the Research Director of electronics of power, intelligent techniques of control and robotics with the Electromechanics Department, Mohammadia School of Engineering, Rabat. He is actively engaged in supervising Ph.D.

thesis in electronics field. His research interests include photovoltaic power systems, hybrid power systems, maximum power point trackers, power generation control, power generation economics, predictive control, battery storage plants, diesel-electric generators, diesel-electric power stations, electric current control, electrolytic devices, energy consumption, energy management systems, field programmable gate arrays, hydrogen production, optimisation, sensors, solar cell arrays, stability, wind power plants, distributed power generation, electric generators, electromagnetic interference, energy storage, and filtering theory.

...